

Free propagation of resonant waves in nonlinear dissipative metamaterials

Research

Cite this article: Fortunati A, Arena A, Lepidi M, Bacigalupo A, Lacarbonara W. 2024 Free propagation of resonant waves in nonlinear dissipative metamaterials. *Proc. R. Soc. A* **480**: 20230759. <https://doi.org/10.1098/rspa.2023.0759>

Keywords:

mechanical metamaterials, nonlinear damping, internal resonances, resonant normal forms, nonlinear waves

Author for correspondence:


Alessandro Fortunati
e-mail: alessandro.fortunati@unina.it

Alessandro Fortunati¹, Andrea Arena², Marco Lepidi³,
Andrea Bacigalupo³ and Walter Lacarbonara²

¹DIETI University of Naples Federico II, Napoli, Italy

²DISG Sapienza University of Rome, Rome, Italy

³DICCA University of Genoa, Genoa, Italy

 AF, 0009-0006-0132-1107; AA, 0000-0003-2411-403X;
ML, 0000-0002-8359-032X; AB, 0000-0002-1266-3907;
WL, 0000-0002-8780-281X

This paper deals with the free propagation problem of resonant and close-to-resonance waves in one-dimensional lattice metamaterials endowed with nonlinearly viscoelastic resonators. The resonators' constitutive and geometric nonlinearities imply a cubic coupling with the lattice. The analytical treatment of the nonlinear wave propagation equations is carried out via a perturbation approach. In particular, after a suitable reformulation of the problem in the Hamiltonian setting, the approach relies on the well-known resonant normal form techniques from Hamiltonian perturbation theory. It is shown how the constructive features of the Lie Series formalism can be exploited in the explicit computation of the approximations of the invariant manifolds. A discussion of the metamaterial dynamic stability, either in the general or in the weak dissipation case, is presented.

1. Introduction

Geometric and constitutive nonlinearities are known to significantly affect the free and forced propagation of mechanical waves in a variety of periodic microstructured media, ranging from granular chains to phononic crystals and mechanical metamaterials [1–4]. From the theoretical point of view, considering the distinctive contribution of different nonlinear sources in physical-mathematical models can substantially enrich the nature and multiplicity of stable solutions resulting from the

governing equations of motion. From a methodological and technical point of view, harnessing the complexity of the nonlinear dynamic phenomena is progressively generating a paradigm shift in the conception and design of new-generation materials [5]. This revolutionary approach opens a wealth of opportunities for an entirely novel realm of functionalities, in which the oscillation amplitude regime is exploited as an extra design variable to trigger and govern hardening/softening behaviours, dispersion modulations, inertial amplifications, superharmonic frequency generations, enhanced dissipation mechanisms, non-reciprocal energy transfers, supertransmission channels, solitary waves propagations and wave interactions [6].

Within this challenging field, an important issue is determining how the wave oscillation amplitude modifies the natural dispersion properties (wavefrequencies, but also waveforms, polarization factors, group velocities and energy flows). From a methodological perspective, suitable analytical solutions to this problem, albeit affected by asymptotic approximations, can be obtained by employing perturbation techniques. This approach aligns with a well-established tradition dating back to the early 1980s [7]. In the past decades, different perturbation methods have been employed to study the nonlinear dispersion properties of harmonic waves in periodic systems, including the ordered Harmonic Balance [8,9], Lindstedt-Poincaré [10–13] and the Method of Multiple Scales [14–18]. Most of the studies in the literature are focused on determining the amplitude-dependent softening or hardening behaviour of the wavefrequency backbone curves. Generally, the key motivation is the possibility to regard the oscillation amplitude as an additional designable variable in the parametric optimization of the spectral band structure for ad hoc applications [19–21]. Consequently, less attention has been devoted to exploring the full potential of perturbation methods in assessing the amplitude-dependent waveforms and/or determining the invariant manifolds in which stable harmonic motions may develop [22–24]. Interest in the nonlinear dynamic phenomena associated with integer or quasi-integer ratios between multiple wave frequencies, leading to internal resonances or near-resonances, has been relatively limited. In particular, there are only a few studies, primarily utilizing the Method of Multiple Scales, dedicated to: (i) describing the emergence of subharmonic bandgaps in the dispersion spectrum of mechanical metamaterials, resulting from autoparametric mechanisms that excite the local resonators [25]; (ii) analyse the quadratic and/or cubic interactions between two internally resonant acoustic waves propagating with different wavelengths in a nonlinear monoatomic lattice [15,26]; (iii) discuss the localization and exchange of mechanical energy between a pair of resonant high-frequency or low-frequency modes of a cubic diatomic finite-size lattice [27]; (iv) study the amplitude modulation, stability and energy transfers between internally resonant waves in weakly nonlinear lattices and metamaterials [28]; (v) determine the nonlinear wavefrequencies and waveforms of a diatomic metamaterial equipped with cubic undamped local resonators under a superharmonic internal resonance between the acoustic and optical waves [23].

Upon examining the current state of the art on nonlinear harmonic wave propagation in periodic systems, it becomes evident that a significant portion of the existing perturbation techniques mostly leverage the dispersion characteristics of the linear undamped system when crafting their foundational (lowest order) solutions to construct more intricate nonlinear (higher order) solutions. This approach aligns with conventional assumptions centred around the presence of weak nonlinearities and minimal or negligible damping effects. In a recent contribution by Fortunati *et al.* [29], the nonlinear dispersion properties of a locally resonant metamaterial endowed with cubic stiffness and damping were described by adopting an extended Hamiltonian perturbation technique, borrowed from the field of Celestial Mechanics. Specifically, a perturbation scheme based on Lie series operators (see, e.g. [30]) was devised to asymptotically approximate the free wave propagation up to the lowest significant perturbation order, under the assumption of non-resonance conditions. Distinguishing itself through its unique methodological approach, the implemented perturbation scheme operates on the premise of using the dispersion characteristics inherent to the linear damped system to create generating solutions at the lowest order. The resulting nonlinear spectra are then elegantly derived as

analytical functions, exhibiting a characteristic exponential decay from their initial values, all in relation to the mechanical parameters and the time-dependent oscillation amplitudes.

Based on this background, the principal objective of the present paper is to remove the simplifying hypothesis of *non-resonant* waves, thus applying the Hamiltonian perturbation scheme to the particular cases of internally resonant waves with acoustic-to-optical wavefrequency ratios 1:3.

2. Hamiltonian perturbation theory

Hamiltonian perturbation theory is typically concerned with the class of dynamic nearly-integrable problems governed by the Hamiltonian

$$H = H_0 + \varepsilon K, \quad (2.1)$$

where H_0 is integrable in the classical sense (à la Arnold–Liouville) and ε is a ‘small’ parameter in such a way the function K plays the role of ‘perturbation’. Either H_0 or K are assumed to be smooth functions. The task consists in finding a *canonical* transformation \mathcal{T} of variables (i.e. a transformation whose Jacobian is a symplectic matrix) in such a way that the transformed Hamiltonian $H' := H \circ \mathcal{T}$ is ‘closer to the integrability than H ’. The precise meaning of this property varies depending on the specific case at hand; however, it is typical to expect $H' - H_0 = O(\varepsilon^2)$. Nevertheless, there are classes of problems—including the resonant case treated in this paper—in which this is not possible. More importantly, a key result of the perturbation theory (see, e.g. [30]) states that, even in the cases in which $H' - H_0 = O(\varepsilon^2)$, the iterative procedure, by which a composition of n transformations (with n arbitrarily large) is sought in such a way that $H^{(n)} - H_0 = O(\varepsilon^{2n})$, is not possible, at least *generically*.

The non-Hamiltonian case can be easily treated by means of the well-established tools of the Hamiltonian approach, simply by observing that a system of ODEs in the form $\dot{x} = v(x)$ with $x \in \mathbb{R}^n$ can be always interpreted as (part of the) canonical equations of the Hamiltonian system

$$\mathcal{H} := \mathbf{y} \cdot \mathbf{v}(x), \quad (2.2)$$

in the extended phase space $\mathbb{M} \ni (x, \mathbf{y})$, with $\mathbb{M} \subset \mathbb{R}^{2n}$, as shown, for instance, in [31].

The tools borrowed from the Hamiltonian framework are not limited to the perturbation scheme, but they also involve some sets of coordinates usually used in this context in order to simplify the form of the normalized equations, as well as to exploit their geometrical meaning, as already shown in [29]. More specifically, the main tool employed to construct canonical transformations consists in the *Lie series operator*

$$\exp(\mathcal{L}_g) := \text{Id} + \sum_{s=1}^{+\infty} \frac{1}{s!} \mathcal{L}_g^s, \quad g \in \mathfrak{G}, \quad (2.3)$$

where $\mathcal{L}_\chi \cdot := \{\cdot, \chi\}$, \mathfrak{G} is the space of smooth functions defined on \mathbb{M} , and

$$\{\hat{f}, \hat{g}\} \equiv \sum_{i=1}^n \left[\partial_{x_i} \hat{f} \partial_{y_i} \hat{g} - \partial_{y_i} \hat{f} \partial_{x_i} \hat{g} \right], \quad \forall \hat{f}, \hat{g} \in \mathfrak{G}, \quad (2.4)$$

are the classical Poisson brackets.

A basic result of the theory of Lie series operators consists in the possibility of proving that the associated transformation of variables

$$(\mathbf{y}, x) := \exp(\mathcal{L}_g)(\mathbf{Y}, X), \quad (2.5)$$

is canonical, see, e.g. [30]. However, the main advantage of this approach with respect to the classical *generating function method* is that the transformation (2.5) possesses an explicit form, so that no inversions are required. This has a remarkable impact in applications involving machine-based implementations of the method leading to several remarkable uses especially in the field of Celestial Mechanics (see, for instance [32]).

and possesses four non-purely imaginary eigenvalues in the form

$$\lambda_{1,2} = \alpha_1 \pm i\beta_1 \quad \text{and} \quad \lambda_{3,4} = \alpha_2 \pm i\beta_2, \quad (3.4)$$

as long as $m \in \mathbb{R}^+$. Furthermore $\alpha_{1,2} < 0$ and – if m is sufficiently small (under damped systems, see also §4a), also $\beta_{1,2} \in \mathbb{R}^+$, so that $\lambda_j \in \mathbb{C} \setminus \{0\}$. From the physical viewpoint, the real and imaginary parts $\alpha_{1,2}$ and $\beta_{1,2}$ can be regarded as *damping ratio* and *frequency* of the acoustic (subscript 1) and optical (subscript 2) branches of the complex-valued dispersion spectrum.

After the determination of a basis of eigenvectors \mathbf{v}_j for \mathbf{A} , which can be properly normalized to have unitary z_1 -component in the form

$$\mathbf{v}_j := \left(1, \lambda_j^{-2}(2l - 2gl - g\lambda_j^2), -\lambda_j^{-1}2l, \lambda_j^{-1}(2l + \lambda_j^2) \right)^\top, \quad (3.5)$$

it is possible to introduce a set of normal coordinates \mathbf{x} and to apply the change of coordinates

$$\mathbf{z} = \mathbf{C}\mathbf{x} \quad \text{and} \quad \mathbf{C} = (\mathbf{v}_1, \mathbf{v}_2, \mathbf{v}_3, \mathbf{v}_4), \quad (3.6)$$

casting the linear part of system (3.1) in the canonical diagonal form

$$\dot{\mathbf{x}} = \mathbf{A}\mathbf{x} + \varepsilon\mathbf{f}(\mathbf{x}), \quad (3.7)$$

where $\mathbf{A} = \text{diag}(\lambda_1, \lambda_2, \lambda_3, \lambda_4)$. Neglecting higher order terms, the vector of cubic nonlinearities reads

$$\mathbf{f}(\mathbf{x}) := \mathbf{C}^{-1}(0, 0, 0, \mathbf{g}^{[\leq 3]}(\mathbf{C}\mathbf{x}))^\top =: \mathbf{g}^{[\leq 3]}(\mathbf{C}\mathbf{x})(r_1, r_2, r_3, r_4)^\top,$$

where the complex coefficients $r_1 = \bar{r}_2$ and $r_3 = \bar{r}_4$ appear. Note that the overbar stands for the complex-conjugate.

(a) A first-order perturbation analysis

Starting from the governing equation (3.7), it is possible to extend the phase space according to the Hamiltonian perturbation theory and define the Hamiltonian function

$$H(\mathbf{y}, \mathbf{x}) := \sum_{j=1}^4 \lambda_j y_j x_j + \varepsilon \tilde{\mathbf{g}}(\mathbf{x}) \sum_{j=1}^4 r_j y_j, \quad (3.8)$$

where, in the ε -scaled perturbation term, the quantity

$$\tilde{\mathbf{g}}(\mathbf{x}) := \mathbf{g}^{[\leq 3]}(\mathbf{C}\mathbf{x}) = \sum_{|\mathbf{v}|=3} \gamma_{\mathbf{v}} P_{\mathbf{v}}(\mathbf{x}), \quad P_{\mathbf{v}}(\mathbf{x}) := \prod_{j=1}^4 x_j^{v_j}, \quad (3.9)$$

with the multi-index $\mathbf{v} \in \mathbb{N}^4$ and $|\mathbf{v}| = v_1 + \dots + v_4$. The explicit form of the coefficients $\gamma_{\mathbf{v}}$ is reported in Appendix B. It is immediate to check that the first set of canonical equations

$$\dot{x}_j := \partial_{y_j} H, \quad \dot{y}_j := -\partial_{x_j} H, \quad (3.10)$$

gives exactly the governing equations (3.7) as $j = 1, \dots, 4$.

According to the classical strategy, a transformation of variables apt to remove ‘as many terms as possible’ from the perturbation term has to be constructed. The procedure outlined in [29] reduces the problem to solving the *homological equation*

$$\{\chi, \sum_{j=1}^4 \lambda_j y_j x_j\} = \tilde{\mathbf{g}}(\mathbf{x}) \sum_{j=1}^4 r_j y_j, \quad (3.11)$$

where the *generating function* of the transformation χ is sought of the form

$$\chi = \varepsilon \sum_{j=1}^4 y_j \sum_{|\mathbf{v}|=3} c_{\mathbf{v}}^{(j)} P_{\mathbf{v}}(\mathbf{x}), \quad (3.12)$$

in which the coefficients $c_v^{(j)}$ play the role of unknowns. According to [35], it is possible to prove that this particular form for χ is the most general choice for Hamiltonians defined as in (3.8).

By substituting the solution (3.12) in equation (3.11), the unknowns $c_v^{(j)}$ are obtained in closed form, as analytical functions of the Taylor series coefficients of the perturbation

$$c_v^{(j)} = \frac{r_j \gamma_v}{\lambda \cdot v - \lambda_j}. \quad (3.13)$$

As a minor observation, it is worth noting that equation (3.13) can be derived through various formulations that do not rely on the Hamiltonian formalism (see, e.g. [36] for a direct construction).

4. Resonant normal form

For the specific problem under investigation, it must be first remarked that solution (3.13) might present particular vectors v for some j such that the denominator, or *divisor* $\lambda \cdot v - \lambda_j$ is zero, regardless of the value of the frequencies. Generally, this happens when the locus of commensurable frequency pairs $\Pi_{i,j}(\sigma) := \{(\beta_1, \beta_2) \in [0, +\infty)^2 : \beta_i = \sigma \beta_j, \text{ with } \sigma \in \mathbb{Q}\}$ belongs to the internal resonance manifold $\mathfrak{R} := \Pi_{2,1}(0) \cup \Pi_{2,1}(1/3) \cup \Pi_{2,1}(1) \cup \Pi_{2,1}(3) \cup \Pi_{1,2}(0)$. Specifically, it is possible to find exactly eight vectors v nullifying the divisor for $(\beta_1, \beta_2) \in \Pi_{2,1}(0)$. Furthermore, four other vectors v make the divisor vanish for $(\beta_1, \beta_2) \in \Pi_{2,1}(1/3)$, that is, for a one-to-three internal resonance. Considering simultaneously both possibilities, the set \mathcal{S}_r of v -values leading to zero divisors is collected in table 1. The issue concerning the physical activation of the internal resonance is discussed in the next section. By excluding zero divisors, we can ascertain that the generating function (3.12) can take the form:

$$\chi = \varepsilon \sum_{j=1}^4 y_j r_j \left[\sum_{\substack{|v|=3 \\ v \notin \mathcal{S}_r}} \frac{\gamma_v P_v(x)}{(\lambda \cdot v - \lambda_j)} \right], \quad (4.1)$$

so that the normalized Hamiltonian $\tilde{H} := \exp(\mathcal{L}_\chi)H$ reads

$$\begin{aligned} \tilde{H} = & \sum_{j=1}^4 \lambda_j Y_j X_j + \varepsilon r_1 Y_1 (\gamma_{(1,0,1,1)} X_1 X_3 X_4 + \gamma_{(2,1,0,0)} X_1^2 X_2 + \gamma_{(0,2,1,0)} X_2^2 X_3) \\ & + \varepsilon r_2 Y_2 (\gamma_{(0,1,1,1)} X_2 X_3 X_4 + \gamma_{(1,2,0,0)} X_1 X_2^2 + \gamma_{(2,0,0,1)} X_1^2 X_4) \\ & + \varepsilon r_3 Y_3 (\gamma_{(0,0,2,1)} X_3^2 X_4 + \gamma_{(1,1,1,0)} X_1 X_2 X_3 + \gamma_{(3,0,0,0)} X_1^3) \\ & + \varepsilon r_4 Y_4 (\gamma_{(0,0,1,2)} X_3 X_4^2 + \gamma_{(1,1,0,1)} X_1 X_2 X_4 + \gamma_{(0,3,0,0)} X_2^3) + O(\varepsilon^2), \end{aligned} \quad (4.2)$$

which is equivalent, by the Gröbner Exchange Theorem, to the original Hamiltonian subject to the transformation via the canonical map $\mathcal{N}_{(x,y) \rightarrow (X,Y)}$ in the form

$$(x, y) = \mathcal{L}_\chi(x, y)|_{(x,y)=(X,Y)} + O(\varepsilon^2). \quad (4.3)$$

The canonical equations associated with such a normal form are

$$\dot{X}_1 = \lambda_1 X_1 + \varepsilon [\Gamma_{(1,0,1,1,1)} X_1 X_3 X_4 + \Gamma_{(2,1,0,0,1)} X_1^2 X_2 + \Gamma_{(0,2,1,0,1)} X_2^2 X_3], \quad (4.4a)$$

$$\dot{X}_2 = \lambda_2 X_2 + \varepsilon [\Gamma_{(0,1,1,1,2)} X_2 X_3 X_4 + \Gamma_{(1,2,0,0,2)} X_1 X_2^2 + \Gamma_{(2,0,0,1,2)} X_1^2 X_4], \quad (4.4b)$$

$$\dot{X}_3 = \lambda_3 X_3 + \varepsilon [\Gamma_{(0,0,2,1,3)} X_3^2 X_4 + \Gamma_{(1,1,1,0,3)} X_1 X_2 X_3 + \Gamma_{(3,0,0,0,3)} X_1^3], \quad (4.4c)$$

and
$$\dot{X}_4 = \lambda_4 X_4 + \varepsilon [\Gamma_{(0,0,1,2,4)} X_2 X_3 X_4 + \Gamma_{(1,1,0,1,4)} X_1 X_2 X_4 + \Gamma_{(0,3,0,0,4)} X_2^3], \quad (4.4d)$$

where $\Gamma_{(i,j,k,l,m)} := \gamma_{(i,j,k,l)} r_m$. For the sake of convenience, the set of standard transformation of variables $\mathcal{R}_{X \rightarrow V}$ is introduced in the form

$$\begin{pmatrix} X_{2j-1} \\ X_{2j} \end{pmatrix} = \frac{1}{\sqrt{2}} \begin{pmatrix} 1 & i \\ 1 & -i \end{pmatrix} \begin{pmatrix} V_{2j-1} \\ V_{2j} \end{pmatrix}, \quad j=1,2, \quad (4.5)$$

to cast the previous system of equations in its real-valued form

$$\begin{aligned} \dot{V}_1 = & \alpha_1 V_1 - \beta_1 V_2 + \frac{1}{2}\varepsilon \left[(M_{1,2}^{(1)} V_1 - N_{1,2}^{(1)} V_2)(V_1^2 + V_2^2) + (M_{3,4}^{(1)} V_1 - N_{3,4}^{(1)} V_2)(V_3^2 + V_4^2) \right. \\ & \left. + M_5(V_1^2 V_3 - V_2^2 V_3 + V_1 V_2 V_4) - N_5(V_1^2 V_4 - V_2^2 V_4 - V_1 V_2 V_3) \right], \end{aligned} \quad (4.6a)$$

$$\begin{aligned} \dot{V}_2 = & \beta_1 V_1 - \alpha_1 V_2 + \frac{1}{2}\varepsilon \left[(N_{1,2}^{(2)} V_3 + M_{1,2}^{(2)} V_4)(V_1^2 + V_2^2) + (N_{3,4}^{(2)} V_3 + M_{3,4}^{(2)} V_4)(V_3^2 + V_4^2) \right. \\ & \left. + N_6 V_1(3V_2^2 - V_1^2) + M_6 V_2(3V_1^2 - V_2^2) \right], \end{aligned} \quad (4.6b)$$

$$\begin{aligned} \dot{V}_3 = & \alpha_2 V_3 - \beta_2 V_4 + \frac{1}{2}\varepsilon \left[(M_{1,2}^{(2)} V_3 - N_{1,2}^{(2)} V_4)(V_1^2 + V_2^2) + (M_{3,4}^{(2)} V_3 - N_{3,4}^{(2)} V_4)(V_3^2 + V_4^2) \right. \\ & \left. + M_6 V_1(V_1^2 - 3V_2^2) + N_6 V_2(3V_1^2 - V_2^2) \right], \end{aligned} \quad (4.6c)$$

and
$$\begin{aligned} \dot{V}_4 = & \beta_2 V_3 + \alpha_2 V_4 + \frac{1}{2}\varepsilon \left[(N_{1,2}^{(2)} V_3 + M_{1,2}^{(2)} V_4)(V_1^2 + V_2^2) + (N_{3,4}^{(2)} V_3 + M_{3,4}^{(2)} V_4)(V_3^2 + V_4^2) \right. \\ & \left. + N_6 V_1(3V_2^2 - V_1^2) + M_6 V_2(3V_1^2 - V_2^2) \right], \end{aligned} \quad (4.6d)$$

where the following auxiliary quantities have been introduced

$$\left. \begin{aligned} M_{1,2}^{(1)} &:= \Re \Gamma_{(2,1,0,0,1)}, & N_{1,2}^{(1)} &:= \Im \Gamma_{(2,1,0,0,1)}, & M_5 &:= \Re \Gamma_{(0,2,1,0,1)}, \\ M_{3,4}^{(1)} &:= \Re \Gamma_{(1,0,1,1,1)}, & N_{3,4}^{(1)} &:= \Im \Gamma_{(1,0,1,1,1)}, & M_6 &:= \Re \Gamma_{(0,3,0,0,4)}, \\ M_{1,2}^{(2)} &:= \Re \Gamma_{(1,1,1,0,3)}, & N_{1,2}^{(2)} &:= \Im \Gamma_{(1,1,1,0,3)}, & N_5 &:= \Im \Gamma_{(0,2,1,0,1)} \\ \text{and} & & M_{3,4}^{(2)} &:= \Re \Gamma_{(0,0,2,1,3)}, & N_{3,4}^{(2)} &:= \Im \Gamma_{(0,0,2,1,3)}, & N_6 &:= \Im \Gamma_{(0,3,0,0,4)}. \end{aligned} \right\} \quad (4.7)$$

Therefore, by employing the change of variables

$$(V_{2j-1}, V_{2j}) = e^{\alpha_j t} (U_{2j-1}, U_{2j}), \quad j=1,2, \quad (4.8)$$

and introducing the so-called *action-angle* coordinates $(\mathbf{I}, \boldsymbol{\varphi})$ through the variable transformation $\mathcal{A}_{\mathbf{U} \rightarrow (\mathbf{I}, \boldsymbol{\varphi})}$ defined as

$$(U_{2j-1}, U_{2j}) = \sqrt{2I_j} (\cos \varphi_j, \sin \varphi_j), \quad j=1,2, \quad (4.9)$$

equations (4.6a)-(4.6d) can be expressed in the form

$$\dot{I}_1 = 2\varepsilon I_1 \left[M_{1,2}^{(1)} I_1 e^{2\alpha_1 t} + M_{3,4}^{(1)} I_2 e^{2\alpha_2 t} \right] - 2\varepsilon \sqrt{I_1^3 I_2} [N_5 \sin \theta_1 - M_5 \cos \theta_1] e^{(\alpha_1 + \alpha_2)t}, \quad (4.10a)$$

$$\dot{\varphi}_1 = \beta_1 + \varepsilon \left[N_{1,2}^{(1)} I_1 e^{2\alpha_1 t} + N_{3,4}^{(1)} I_2 e^{2\alpha_2 t} \right] + 2\varepsilon \sqrt{I_1^3 I_2} [M_5 \sin \theta_1 + N_5 \cos \theta_1] e^{(\alpha_1 + \alpha_2)t}, \quad (4.10b)$$

$$\dot{I}_2 = 2\varepsilon I_2 \left[M_{1,2}^{(2)} I_1 e^{2\alpha_1 t} + M_{3,4}^{(2)} I_2 e^{2\alpha_2 t} \right] - 2\varepsilon \sqrt{I_1^3 I_2} [N_6 \sin \theta_1 - M_6 \cos \theta_1] e^{(\alpha_1 + \alpha_2)t} \quad (4.10c)$$

and
$$\dot{\varphi}_2 = \beta_2 + \varepsilon \left[N_{1,2}^{(2)} I_1 e^{2\alpha_1 t} + N_{3,4}^{(2)} I_2 e^{2\alpha_2 t} \right] - \varepsilon \sqrt{I_1^3 I_2} [M_6 \sin \theta_1 + N_6 \cos \theta_1] e^{(3\alpha_1 - \alpha_2)t}, \quad (4.10d)$$

where the angle coordinates have been reparameterized by introducing the positions

$$\theta_1 = -3\varphi_1 + \varphi_2 \quad \text{and} \quad \theta_2 = \varphi_2. \quad (4.11)$$

As a complementary remark, it can be noted that the choice $\theta_2 = \varphi_2$ is quite arbitrary and it is assumed here for the sake of simplicity. In general, any other linearly independent combination of angles with respect to the coefficient pair $(-3, 1)$ would work. The same is not true in the Hamiltonian case (i.e. if a symplectic transformation is required). As for the latter, a general

Table 1. The set \mathcal{S}_j of \mathbf{v} leading to a zero divisor.

j	\mathbf{v} for $\Pi_{2,1}(0)$	\mathbf{v} for $\Pi_{2,1}(1/3)$
1	(1,0,1,1), (2,1,0,0)	(0,2,1,0)
2	(0,1,1,1), (1,2,0,0)	(2,0,0,1)
3	(0,0,2,1), (1,1,1,0)	(3,0,0,0)
4	(0,0,1,2), (1,1,0,1)	(0,3,0,0)

criterion to choose such a transformation is described, e.g. in [37]. It is interesting to compare the set of equations (4.10a)–(4.10d) obtained above with [29, Eqs. (33)], i.e. the equations found in the non-resonant case. In particular, it is immediately noticed that, in this case, some $O(\varepsilon)$ extra terms appear in the right-hand side of (4.10a)–(4.10d). The latter carries the contribution of the selected 1 : 3 resonance, breaking in this way the remarkable independence upon the angles which characterizes the related set in [29]. Hence, compared to the non-resonant case equations (4.10a)–(4.10d) depend on four further functions $M_{5,6}$ and $N_{5,6}$, besides $M_{1,2}^{(1,2)}$ and $N_{1,2}^{(1,2)}$. The behaviour of this whole set of functions is depicted in figure 2 as d and h vary. All the functions appear to depend almost linearly on the varying parameters. Furthermore, the functions can attain either positive or negative values, with change of sign in the closeness of $d = 0$.

(a) Resonant loci

The physical activation of the one-to-three internal resonance needs some discussion. To this end, the governing matrix A has been demonstrated to possess four, pairwise complex-conjugate, eigenvalues of the form $\alpha_{1,2} \pm i\beta_{1,2}$, for any set of parameters g, l, μ , and sufficiently small m . Moreover, the following first-order expressions have been proved:

$$\alpha_{1,2}^{[\leq 1]} = -m[g\mathcal{D} \mp (gl - 2l - g^2\mu)]/(4\mathcal{D}), \quad \beta_{1,2}^{[\leq 1]} = \sqrt{\mu g + l} \mp \mathcal{D}, \quad (4.12)$$

where $\mathcal{D} := \sqrt{(\mu g + l)^2 + 4l\mu(1 - g)}$. The associated proofs can be found in [29, Prop.2.1 and Prop.5.1].

Remark 4.1. It is possible to show that $\alpha_{1,2}^{[\leq 1]} = 0$ if $m = 0$ via a Routh–Hurwitz argument, see [29, Prop.2.1].

The theoretical issue to be addressed is the existence and analytical definition of *resonant loci*, that is, parameter combinations that realize one-to-three internal resonances between the metamaterial frequencies $\beta_{1,2}$. Another important consideration deals with devising an algorithmic procedure for approximating the spectrum of the resonant metamaterial. In pursuit of this objective, we can outline the following

Proposition 4.2 (Existence of nearly resonant 1 : 3 eigenvalues). *Based on the definition of matrix A as in equation (3.3), let us choose the parameter μ in the form*

$$\mu = l(16 - \kappa^2)/9, \quad \kappa \in (\sqrt{346}/5, 4), \quad (4.13)$$

where κ is an auxiliary positive real parameter used to parameterize μ . Then, for any value of the coefficient $l \in (0, 1)$, there exist boundary values $m_0 > 0$ and $\delta_0 > 0$ and four functions $\alpha_{1,2}(m), \beta_1(\delta, m), g(\delta, m) \rightarrow \mathbb{R}$ satisfying $\alpha_{1,2}(0) = 0$, and such that $\lambda(\delta, m) := \alpha_j(m) \pm i\beta_j(\delta, m)$ for $j = 1, 2$, are roots of the characteristic equation

$$\det(A - \lambda I) = 0, \quad \forall (\delta, m) \in [0, \delta_0] \times [0, m_0], \quad (4.14)$$

with

$$\beta_2(\delta, m) = (3 + \delta)\beta_1(\delta, m), \quad 3\alpha_1 - \alpha_2 < 0. \quad (4.15)$$

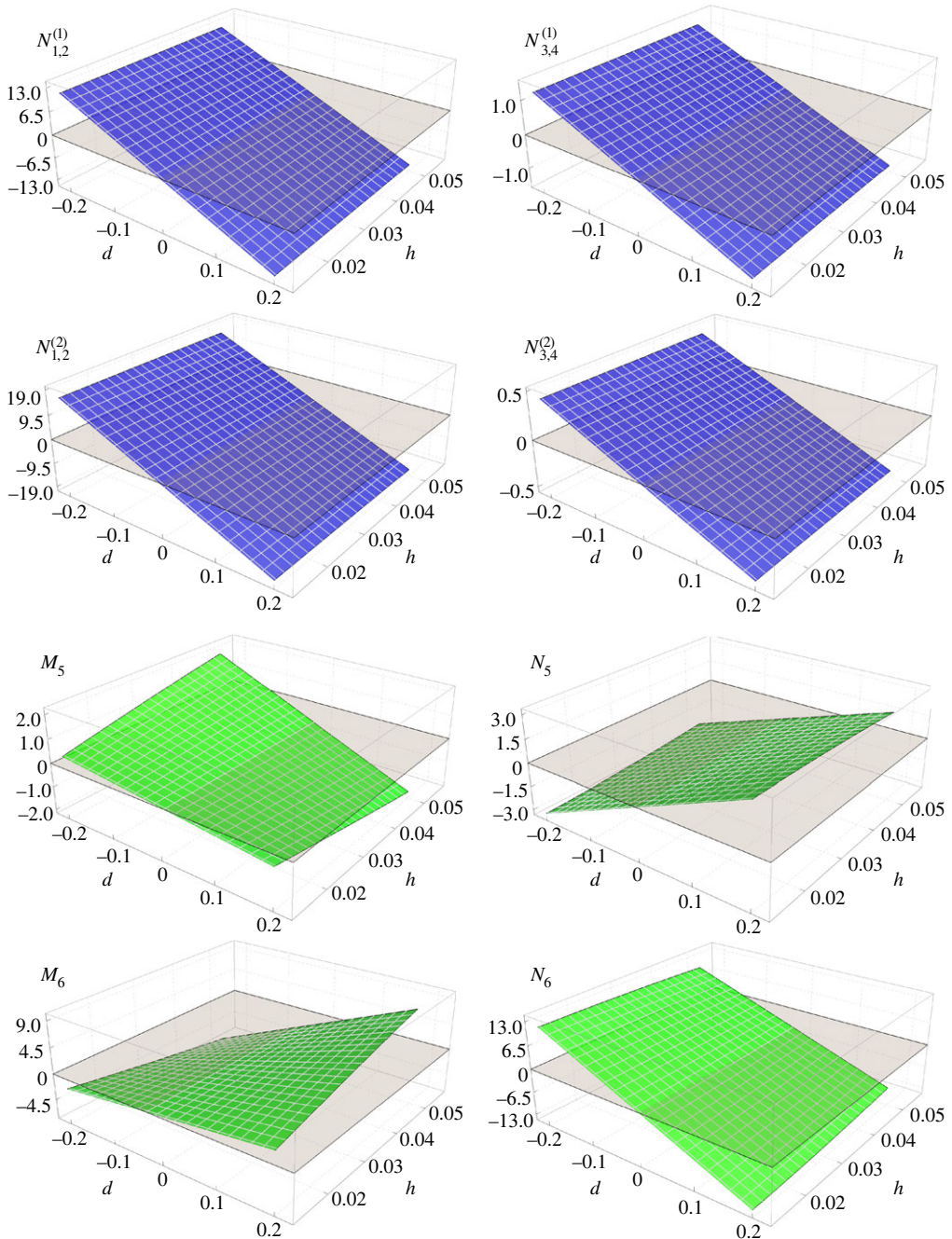


Figure 2. Plots of the coefficients appearing in (4.19) as functions of d and h . These surfaces have been obtained by setting $\beta = \pi/2$ with $\xi_2 = \xi_3 = 0.5$ (the value of ξ_1 is variable because of the variation of h) and $\mu = 0.0867$.

Accordingly, the parameter δ plays the role of internal detuning, and the nearly resonant 1 : 3 eigenvalues can be referred to as δ -resonant eigenvalues. Furthermore, it can be noted that

$$\alpha_{1,2}(m) = \alpha_{1,2}^{[\leq 1]}, \quad (4.16)$$

while either $\beta_1(\delta, m)$ or $g(\delta, m)$ can be determined via a convergent algorithm for all $(\delta, m) \in [0, \delta_0) \times [0, m_0)$.

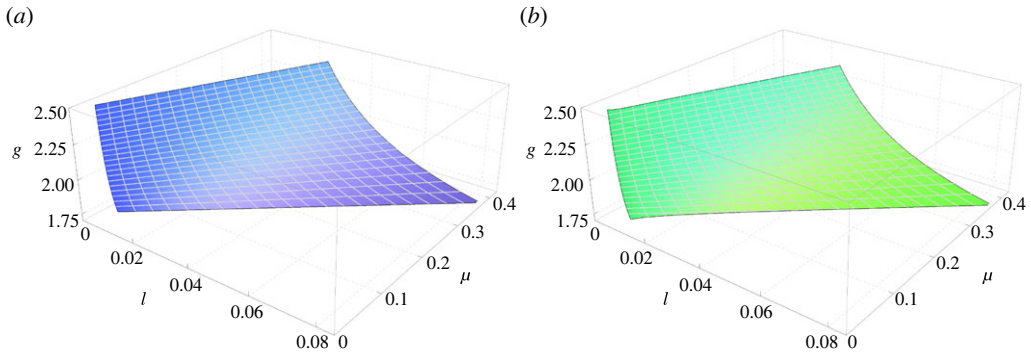


Figure 3. Resonant manifolds constructed by setting: (a) $m = \delta = 0.001$; (b) $m = 0.06$ and $\delta = 0.028$.

The proof of proposition 4.2 is given in Appendix A.

Remark 4.3. Condition (4.15) is essential for the existence of the exponential terms appearing in equation (4.10) for all $t > 0$.

Examples of resonant loci constructed via the algorithm described in Appendix A are presented in figure 3. As mentioned before, the surfaces shown in figure 3 represent the sets of parameters for which the eigenvalues of the system are found to be in a 1 : 3 resonance. As is clear from the caption, those surfaces have been computed for ‘small’ values of m : this possibility is guaranteed by proposition 4.2. It is important to stress that, as the determination of the eigenvalues is reduced to the resolvability of the nonlinear system (A 1), there is no guarantee that, beyond a certain threshold m_0 , a solution to (A 1) would exist in the first place. Furthermore, the proof of proposition 4.2, based on the classical Implicit Function Theorem, provides the (efficient) algorithm (A 4) of a *quasi-Newton* type for the numerical approximation of the mentioned loci.

(b) Nonlinear frequencies

The aim of this section is to give a first-order expression for the nonlinear spectra. First, recalling that $\lambda_j \in \mathbb{C} \setminus \{0\}$, the *detuning parameter* or defect of internal resonance can be expressed as

$$\delta := \beta_1^{-1} \beta_2 - 3, \quad (4.17)$$

and its small variations can be used to span a suitable neighbourhood of the exact 3 : 1 internal resonance. Second, it can be noticed that equations (4.10b) and (4.10d) imply immediately $\dot{\varphi}_j = \beta_j + O(\varepsilon)$, hence the difference

$$\theta_1(t) = 3\varphi_1(t) - \varphi_2(t) = \delta\beta_1 t + O(\varepsilon). \quad (4.18)$$

Third, the solution $I_j(t) = I_j(0) + O(\varepsilon)$ can be immediately obtained from equations (4.10a) and (4.10c). Consequently, equations (4.10b) and (4.10d) finally read:

$$\begin{aligned} \dot{\varphi}_1 = & \beta_1 + \varepsilon [N_{1,2}^{(1)} I_1(0) e^{2\alpha_1 t} + N_{3,4}^{(1)} I_2(0) e^{2\alpha_2 t}] \\ & + 2\varepsilon \sqrt{(I_1(0))^3 I_2(0)} e^{(\alpha_1 + \alpha_2)t} [M_5 \sin(\delta\beta_1 t) + N_5 \cos(\delta\beta_1 t)] + O(\varepsilon^2) \end{aligned} \quad (4.19a)$$

and

$$\begin{aligned} \dot{\varphi}_2 = & \beta_2 + \varepsilon [N_{1,2}^{(2)} I_1(0) e^{2\alpha_1 t} + N_{3,4}^{(2)} I_2(0) e^{2\alpha_2 t}] \\ & - \varepsilon \sqrt{(I_1(0))^3 / I_2(0)} e^{(3\alpha_1 - \alpha_2)t} [M_6 \sin(\delta\beta_1 t) + N_6 \cos(\delta\beta_1 t)] + O(\varepsilon^2) \end{aligned} \quad (4.19b)$$

whose solution is clearly reduced to quadratures up to the first order in ε . By neglecting higher order terms, the uncoupled system of equations (4.19) governs the first-order approximation

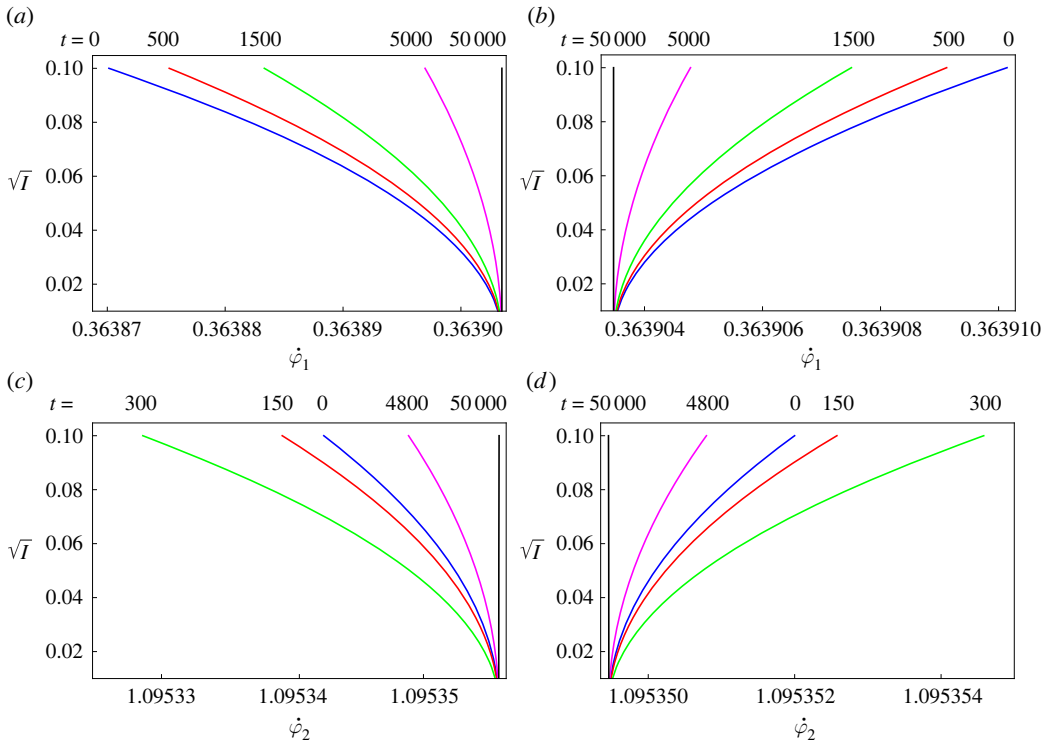


Figure 4. Snapshots of the nonlinear backbone curves at $\beta = \pi$ as a function of $I := \sqrt{l_1^2(0) + l_2^2(0)}$ subjected to the constraint $l_1(0) = l_2(0)$. The properties of the material have been chosen as $\xi_1 = 0.001$, $\xi_2 = \xi_3 = 0.5$, $\mu = 0.0867$. The panels (a) and (c) represent the case $\eta = 0.02$ while (b) and (d) the case $\eta = 0.1$. The values for ε and δ have been set to 0.001 and 0.01, respectively.

of the *nonlinear frequencies* $S_{j,\varepsilon}$ of the metamaterial. Indeed, the time-dependent and internally resonant angles $\varphi_1(t)$ and $\varphi_2(t)$ can be interpreted as nonlinear frequencies, depending on the assigned initial actions $I_1(0)$ and $I_2(0)$ that can be regarded as (square of) initial oscillation amplitudes.

As the main difference with respect to the non-resonant case [29], equation (4.19) is enriched by the ε -order trigonometric terms, whose effects quantitatively depend on the coefficients M_5, N_5, M_6, N_6 . Due to the trigonometric terms $\sin(\delta\beta_1 t)$ and $\cos(\delta\beta_1 t)$, the frequency's dependence on amplitude can manifest as a time-dependent oscillatory behaviour, indicating that the hardening or softening trends do not monotonically diminish with increasing time. The backbone curves are reported in figure 4. Depending on the stiffness parameter d , the backbone curves of both frequencies $\varphi_1(t)$ and $\varphi_2(t)$ can exhibit either a hardening or a softening bending, corresponding to positive stiffness $d > 0$ (figure 4a,c) or negative stiffness $d < 0$ (figure 4b,d), respectively. Specifically, the backbones of frequency φ_2 show the oscillatory behaviour caused by the trigonometric terms (figure 4c,d). However, it should be highlighted that an arbitrarily slow variation with time can be introduced via a suitable reduction of the detuning parameter size, and this allows us to control either the speed or even the occurrence of the above mentioned oscillations. Figure 5 shows the behaviour of the backbones as β varies from zero to $\pi/2$.

5. Weak dissipation and invariant manifolds

Proposition 5.1. *The following properties hold*

$$\left(M_{j_1 j_2}^{(1)}, M_{j_1 j_2}^{(2)}, M_{j_3} \right) = O(m). \quad (5.1)$$

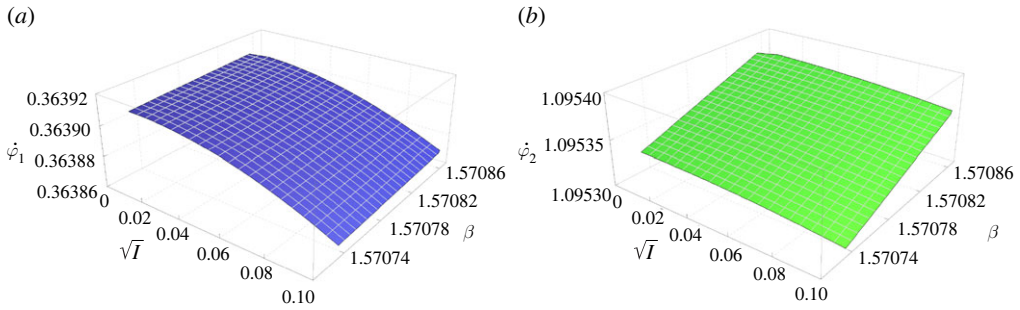


Figure 5. Backbones surfaces providing the frequencies as functions of the amplitude \sqrt{I} and wavenumber β . The material properties and parameter values have been chosen as in figure 4a,c.

Proof. See [29, Prop. 5.1] for $M_{j_1 j_2}^{(1)}$ and $M_{j_1 j_2}^{(2)}$. The proof for M_{j_3} is similar. Another way to prove (5.1) is to check that they vanish for $m = 0$ by (B1), then use their analyticity as functions of m . ■

If one sets $m = O(\varepsilon)$, the system (4.10) reduces, up to $O(\varepsilon)$, to

$$\left. \begin{aligned} \dot{I}_1 &= -2\varepsilon \tilde{N}_5 \sqrt{I_1^3} I_2 \sin \theta_1, \\ \dot{I}_2 &= -2\varepsilon \tilde{N}_6 \sqrt{I_1^3} I_2 \sin \theta_1, \\ \dot{\theta}_1 &= \beta_1 \delta + \varepsilon (\tilde{N}_{1,2}^{(2)} - 3\tilde{N}_{1,2}^{(1)}) I_1 + \varepsilon (\tilde{N}_{3,4}^{(2)} - 3\tilde{N}_{3,4}^{(1)}) I_2 - \varepsilon I_1^{3/2} \left[6\tilde{N}_5 \sqrt{I_2} + \frac{\tilde{N}_6}{\sqrt{I_2}} \right] \cos \theta_1 \end{aligned} \right\} \quad (5.2)$$

and $\dot{\theta}_2 = (3 + \delta)\beta_1 + \varepsilon (\tilde{N}_{1,2}^{(2)} I_1 + \tilde{N}_{3,4}^{(2)} I_2) - \varepsilon \tilde{N}_6 \sqrt{\frac{I_1^3}{I_2}} \cos \theta_1$

where $(\tilde{N}_{j_1}, \tilde{N}_{j_2 j_3}^{(1)}, \tilde{N}_{j_2 j_3}^{(2)}) := (N_{j_1}, N_{j_2 j_3}^{(1)}, N_{j_2 j_3}^{(2)})|_{m=0}$. By using (B1), they are easily computed as

$$\begin{aligned} \tilde{N}_{3,4}^{(1)} &= -3d \Delta_1 \Delta_2^2 [\beta_1 \beta_2^4 (\beta_2^2 - \beta_1^2)]^{-1}, & \tilde{N}_{1,2}^{(2)} &= 3d \Delta_1^2 \Delta_2 [\beta_1^4 \beta_2 (\beta_2^2 - \beta_1^2)]^{-1}, \\ \tilde{N}_{1,2}^{(1)} &= -3d \Delta_1^3 [2\beta_1^5 (\beta_2^2 - \beta_1^2)]^{-1} & \tilde{N}_{3,4}^{(2)} &= 3d \Delta_2^3 [2\beta_2^5 (\beta_2^2 - \beta_1^2)]^{-1} \\ \tilde{N}_5 &= -3d \Delta_1^2 \Delta_2 [2\beta_1^3 \beta_2^2 (\beta_2^2 - \beta_1^2)]^{-1} & \tilde{N}_6 &= -\beta_2 d \Delta_1^3 [2\beta_1^6 (\beta_2^2 - \beta_1^2)]^{-1} \end{aligned}$$

where $\Delta_j := 2(g-1)l - \beta_j^2$.

In order to find the first-order approximation of the invariant manifolds we firstly observe that from the first two equations of (5.2) one gets for all $\tilde{N}_6 \neq 0$

$$I_1 = K_1 + \left(\frac{\tilde{N}_5}{\tilde{N}_6} \right) I_2, \quad K_1 \in \mathbb{R}. \quad (5.3)$$

Let us expand $I_j(t) = I_j^{(0)}(t) + \varepsilon I_j^{(1)}(t) + O(\varepsilon^2)$. First of all, it is immediate that $I_j^{(0)} = \text{const.}$ and $\theta_1(t) = \delta \beta_1 t + O(\varepsilon)$. Hence, from the second of (5.2), one obtains, after performing a quadrature,

$$I_2^{(1)}(t) = -2\tilde{N}_6 (I_1^{(0)})^{3/2} \sqrt{I_2^{(0)}} \left(\frac{\cos(\Theta_1) - \cos(\delta \beta_1 t + \Theta_1)}{\beta_1 \delta} \right), \quad \Theta_1 \in \mathbb{S}^1. \quad (5.4)$$

It is now sufficient to reparameterize the latter as a function of θ_1 and use (5.3) to get the first-order expression of the manifolds in the normalized system. In particular, we get that either I_1 or I_2 depends on θ_1 only, this property will lead to an easily recognizable symmetry in the manifolds plots, as shown, e.g. in figure 6.

Remark 5.2. The limit $\delta \rightarrow 0$ exists in (5.4) and it is the well-known *secular term*, i.e. of the form $t \sin(\Theta_1)$, which is typical of the exact resonance condition. For this reason, in order to ensure that

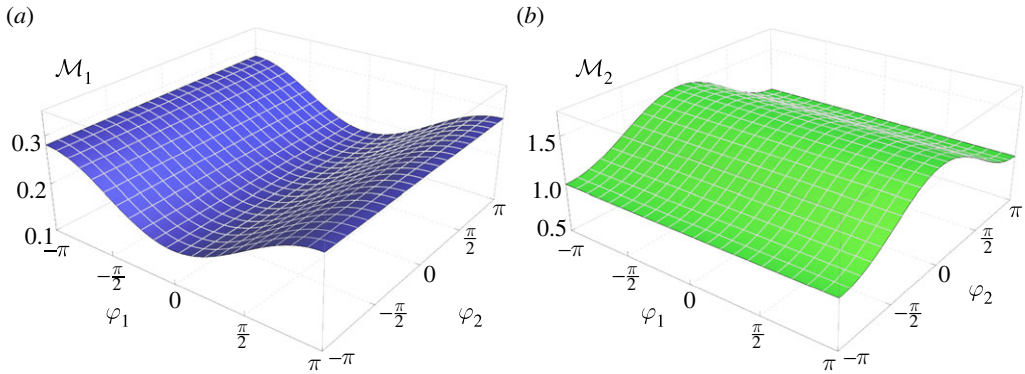


Figure 6. Example of invariant manifolds in the weak dissipation case. The effect of the invariance of the surfaces with respect to space $\theta_1 = \text{const.}$ is notable.

the manifolds exist and, in particular, are graphs of functions, we shall require that $\delta > C\varepsilon^{1-s}$, for all $s \in (0, 1)$.

In other terms, it is possible to represent the invariant manifolds in the normalized system as the two surfaces

$$\tilde{\mathcal{M}}_j := \{I_j(\varphi) : \varphi \in \mathbb{T}^2\}, \quad j = 1, 2,$$

where $I_j(\varphi)$ are defined via (5.3) and the reparameterization of (5.4), with θ_1 as in (4.11) and for some fixed $\theta_1 \in [0, 2\pi]$.

In order to obtain the desired approximation of the invariant manifolds in the original system, it is sufficient to map the surfaces back via the normalizing transformation of variables given by (4.3). More precisely, by defining, for $j = 1, 2$,

$$\mathcal{M}_j := \{((\mathcal{A}_{v \rightarrow (\mathcal{I}, \psi)})^{-1} \circ (\mathcal{R}_{x \rightarrow v})^{-1} \circ \mathcal{N}_{x \rightarrow X} \circ \mathcal{R}_{X \rightarrow V} \circ \mathcal{A}_{V \rightarrow (\mathcal{I}, \varphi)}(\mathcal{I}(\varphi), \varphi))_j, \quad \varphi \in \mathbb{T}^2\},$$

a representation of the invariant manifolds of the original system is obtained. As for the above definition, recall (4.3), (4.5) and (4.9) (note that we have disregarded the transformation defined by (4.8) as it reduces to the identity in the weak dissipation case and for $t = O(1)$).

An example of $\mathcal{M}_{1,2}$ is presented in figure 6.

6. Stability analysis

(a) General case

Let us suppose that m is positive, away from zero and independent from ε . Under the prevailing assumptions, a global result of asymptotic stability holds.

Proposition 6.1. *Suppose $m = O(1)$, $m > 0$ and let*

$$\mathcal{D}_\rho := \{(V_1, \dots, V_4) \in \mathbb{R}^4 : |V_j| < \rho\}.$$

Then, for all $\rho > 0$, there exists $\varepsilon_\rho^ > 0$ such that the system (4.6b) is asymptotically stable on \mathcal{D}_ρ for all $\varepsilon \in (0, \varepsilon_\rho^*)$.*

Proof. (Sketch) Under the assumption $m > 0$, one can obtain from (4.12), (4.16) and remark 4.1 that $\alpha_{1,2} < 0$ hence, it is possible to consider the following function:

$$W := -\alpha_1^{-1}(V_1^2 + V_2^2) - \alpha_2^{-1}(V_3^2 + V_4^2). \quad (6.1)$$

It is easy to check that W is a Lyapunov function for the system (4.6b) on \mathcal{D}_ρ , in particular, $\dot{W} = \sum_{j=1}^4 \dot{V}_j \partial_{V_j} W = -\sum_{j=1}^4 V_j^2 + O(\varepsilon)$. Hence, the latter is strictly negative for all $\rho > 0$, provided that ε is sufficiently small. ■

(b) Weak dissipation case

Proposition 6.1 states that the system is asymptotically stable. However, this property relies on the fact that the dissipation has to be bounded away from zero. The aim of this section is to show that if m approaches zero, some regions of instability may appear.

To this end let us set $\delta =: \varepsilon h$. Either periodic or quasi-periodic solutions of the original system are given, up to the first order in ε , by the equilibrium solutions of (5.2).

Firstly, let us focus on the equilibria for which $I_{1,2}$ are bounded away from zero. By setting $(X, a) := (\sqrt{I_1}, \sqrt{I_2}) \in (0, +\infty)^2$, these equilibria occur if $\theta_1 = k\pi$ with $k \in \mathbb{Z}$, $\theta_2 \in \mathbb{S}^1$ and X is a root of the following equation:

$$-k_3 X^3 \cos \theta_1 + k_2 X^2 + k_0 = 0,$$

where

$$k_3 = a^{-1} \tilde{N}_6 + 6a \tilde{N}_5, \quad k_2 = \tilde{N}_{1,2}^{(2)} - 3\tilde{N}_{1,2}^{(1)}, \quad k_0 = (\tilde{N}_{3,4}^{(2)} - 3\tilde{N}_{3,4}^{(1)})a^2 + \beta_1 h. \quad (6.2)$$

Let $\mathbf{J}^II = \{j_{kl}^{II}\}_{k,l=1,2,3}$ denote the Jacobian matrix (with respect to the variables I_1, I_2, θ_1) of (5.2). In this case, the latter possesses the form

$$j_{kl}^{II} = -\varepsilon \begin{cases} 2\tilde{N}_5 \sqrt{I_1^3 I_2}, & (k, l) = (1, 3) \\ 2\tilde{N}_6 \sqrt{I_1^3 I_2}, & (k, l) = (2, 3) \\ 9\tilde{N}_5 \sqrt{I_1 I_2} + \left(\frac{3}{2}\right) \tilde{N}_6 \sqrt{\frac{I_1}{I_2}} - 3\tilde{N}_{1,2}^{(1)} + \tilde{N}_{1,2}^{(2)}, & (k, l) = (3, 1) \\ 3\tilde{N}_5 \sqrt{\frac{I_1^3}{I_2}} + \left(\frac{1}{2}\right) \tilde{N}_6 \sqrt{\left(\frac{I_1}{I_2}\right)^3} - 3\tilde{N}_{3,4}^{(1)} + \tilde{N}_{3,4}^{(2)}, & (k, l) = (3, 2) \\ 0, & \text{otherwise.} \end{cases}$$

Such a structure has also been found in the paper [38]. The spectrum of such a matrix is easily computed as

$$\text{spec}(\mathbf{J}^II) = \{0, \sqrt{j_{23}^{II} j_{32}^{II}} + j_{13}^{II} j_{31}^{II}, -\sqrt{j_{23}^{II} j_{32}^{II}} + j_{13}^{II} j_{31}^{II}\}.$$

As a consequence, the system cannot be stable if $(j_{23}^{II} j_{32}^{II} + j_{13}^{II} j_{31}^{II}) > 0$. Otherwise, we are in the presence of a *marginally stable* linearization. This implies that no conclusion can be drawn with respect to the stability of the original nonlinear system, see, for instance, [39, p. 386]. We shall refer to this one as a *degenerate* case.

A completely degenerate case is represented by the instance $I_1 = 0$. In this situation, equilibria are given by $(\theta_1, \theta_2) \in \mathbb{T}^2$ and I_2 satisfying the following equation:

$$(3\tilde{N}_{3,4}^{(1)} - \tilde{N}_5)I_2 = \beta_1 h.$$

Let us denote with $\mathbf{J}^I = \{j_{kl}^I\}_{k,l=1,2,3}$ the Jacobian matrix of the obtained system. The latter, evaluated on this set of equilibria, easily yields the following entries:

$$j_{kl}^I = \varepsilon \begin{cases} \tilde{N}_{1,2}^{(2)} - 3\tilde{N}_{1,2}^{(1)}, & (k, l) = (3, 1) \\ \tilde{N}_{3,4}^{(2)} - 3\tilde{N}_{3,4}^{(1)}, & (k, l) = (3, 2) \\ 0, & \text{otherwise} \end{cases}$$

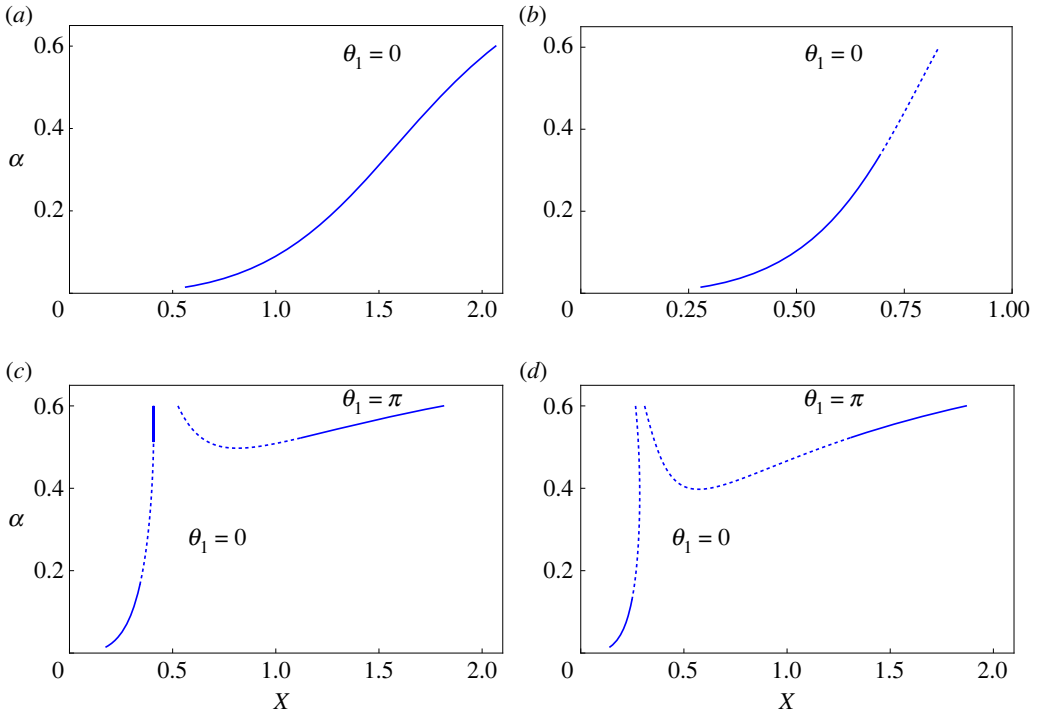


Figure 7. Bifurcation diagram for $\beta = \pi/3$ and different values of μ representing the loci of the equilibria of system (5.2) in the plane (X, a) and their classification: the points belonging to the dashed portions of the branches represent unstable solutions, while the continuous line denotes the (marginally) stable cases. As μ is decreased from the value chosen for (a), a new branch originates in (c) and (d), corresponding to solutions in which $\theta_1 = \pi$ (the periodicity is omitted to simplify the notation). The four values for μ are 0.0496, 0.0475, 0.0433, 0.0402, respectively. The material properties have been set as in figure 4 with the exception of $\xi_1 = \varepsilon = 0.001$ in order to obtain $m = O(\varepsilon)$. Furthermore, we have set $h = 1$, i.e. $\delta = \varepsilon$ and $\eta = 0.05$.

which clearly possesses the null eigenvalue only, with a multiplicity equal to three. The loci of the equilibria of system (5.2) in the plane (X, a) and their transitions from the (marginally) stable case to the unstable case are depicted in the bifurcation diagram of figure 7. The panels describe four different values of μ . It is clear that a variation of μ not only affects the stability of the solutions but can also give rise to new branches of equilibria, as in (c) and (d).

7. Conclusion

This study addresses the intriguing problem of free wave propagation in nonlinear dissipative mechanical metamaterials that incorporate viscoelastic resonators in their periodic cells. More specifically, our investigation is focused on phenomena associated with waves characterized by a nearly 1:3 acoustic-to-optical frequency ratio which entails an internal (autoparametric) resonance. This special internal resonance scenario between the acoustic and the optical waves has deep implications on the bandgap behaviour of metamaterials for which the design variables allow a suitable tuning.

Our work builds upon and complements the findings presented in [29], where a perturbative approach was employed within a non-resonant context. To advance our analysis, we first employ a conventional phase space extension, a technique that has proven its utility in [29]. Subsequently, we apply a suite of tools and methodologies rooted in Hamiltonian resonant normal forms to successfully approximate the nonlinear frequency-wavenumber dependence on wave amplitudes and the invariant manifolds of our one-dimensional metamaterial.

A notable advantage of the Hamiltonian formulation adopted in this study lies in its capacity to accommodate perturbation analyses of arbitrarily high order. This versatility is made possible by leveraging a comprehensive formulation rooted in the contexts of Lie series and Lie transforms.

The equations arising from our resonant normal form are compared directly to those derived in the non-resonant scenario as presented in [29]. Notably, our equations include an additional term that characterizes waves in close proximity to the internal resonance. This extra term is responsible for the well-known secular terms, particularly evident when the distance from the resonant manifold approaches zero.

The perturbative scheme proposed in this work allows an accurate description of the propagation of Bloch waves in lattice metamaterials with periodic microstructure and potentially complex topologies. The approach offers a concise characterization of the dispersion properties of such waves, by exploiting the key physical aspects of the problem at hand. The outcomes can be useful for the conceptualization, design and optimization of smart acoustic waveguides as well as tunable metafilters for advanced technological and engineering applications. More specifically, it is possible to customize the mechanical properties of the nonlinear metamaterial with the aim of slowing down the nonlinear wave propagation (hardening case for heavy metamaterials) or speeding it up (softening case for light ones). The goal is to increase or reduce the effect of those nonlinear effects via a suitable tuning of the dissipation of the metamaterial.

As an ancillary outcome of our investigation, we establish a criterion for the existence of resonant loci, especially valid for sufficiently small dissipation values. Moreover, we offer an efficient numerical algorithm for approximating these loci as a valuable by-product of this work.

Data accessibility. This article has no additional data.

Declaration of AI use. We have not used AI-assisted technologies in creating this article.

Authors' contributions. A.F.: conceptualization, formal analysis, investigation, methodology, software, visualization, writing—original draft; A.A.: conceptualization, formal analysis, methodology, writing—review and editing; M.L.: conceptualization, formal analysis, methodology, writing—review and editing; A.B.: conceptualization, formal analysis, methodology, writing—review and editing; W.L.: conceptualization, funding acquisition, methodology, project administration, resources, supervision, writing—review and editing.

All authors gave final approval for publication and agreed to be held accountable for the work performed therein.

Conflict of interest declaration. We declare we have no competing interests.

Funding. AF gratefully acknowledges the support of the Italian Ministry of Education, University and Scientific Research under PRIN Grant No. 2017L7X3CS at the University of Rome 'La Sapienza', under which the research was carried out, the paper conceptualized and written, as well as the Italian Ministry of University and Research, PRIN2020 funding program, grant number 2020PY8KTC at the University of Naples Federico II which supported him during the revision of the paper. WL gratefully acknowledges the financial support of the Air Force Office of Scientific Research, Grant No. FA 8655-20-1-7025. Moreover, the authors acknowledge the partial support of the National Group of Mathematical Physics (GNFM-INdAM), from the Compagnia SanPaolo, project MINIERA no. I34I20000380007 and from the University of Trento, project UNMASKED 2020.

Appendix A

(a) Proof of proposition 4.2

Given A , eigenvalues of the form $a_{1,2} \pm i\sqrt{b_{1,2}}$ are solutions of the characteristic equation for A if they satisfy the following system of nonlinear equations:

$$\left. \begin{aligned} a_1 + a_2 &= -mg, \\ a_1^2 + 4a_1a_2 + a_2^2 + b_1 + b_2 &= 2(\mu g + l), \\ a_1b_2 + a_1a_2^2 + (b_1 + a_1^2)a_2 &= -(g - 1)lm, \\ a_1^2a_2^2 + a_1^2b_1 + a_2^2b_2 + b_1b_2 &= 4l\mu(g - 1). \end{aligned} \right\} \quad (\text{A } 1)$$

and

Given the expressions, let

$$a_{1,2} = \alpha_{1,2}^{[\leq 1]} + \sum_{n \geq 2} a_{1,2}^{(n)} m^n, \quad b_{1,2} = (\beta_{1,2}^{[\leq 1]})^2 + \sum_{n \geq 2} b_{1,2}^{(n)} m^n.$$

By substituting the above expansions into (A 1), it is not difficult to check by induction that, in particular, $\alpha_{1,2}^{(n)} = 0$ for all $n \geq 2$. This proves (4.16).

Let us now substitute the first of (A 1) into the remaining equations, then define

$$\gamma := (3 + \delta)^2. \quad (\text{A } 2)$$

By setting $b_2 = \gamma b_1$ and defining

$$F_1 := (\gamma + 1)b_1 - 2(g\mu + l) + 4^{-1}(g^2 m^2) - gma_2 - 2a_2^2$$

$$F_2 := 2^{-1}b_1 g m \gamma + b_1 a_2 \gamma - 4^{-1}a_2 g^2 m^2 - (g - 1)lm - 2^{-1}a_2^2 g m - b_1 a_2$$

$$F_3 := 4^{-1}b_1 g^2 m^2 \gamma + b_1 a_2 g m \gamma + b_1 a_2^2 \gamma + b_1^2 \gamma - 4(g - 1)lm\mu + 4^{-1}a_2^2 g^2 m^2 + a_2^3 g m + a_2^4 + b_1 a_2^2,$$

where $F_j := F_j(a_2, b_1, g; l, \mu, \gamma, m)$, system (A 1) turns out to be equivalent to the condition $F = \mathbf{0}$. In order to satisfy the latter, let us firstly observe that, as $\alpha_2^{[\leq 1]}$ and $\beta_1^{[\leq 1]}$ are solutions to (A 1) up to the first order in m , we get

$$F_j(\alpha_2^{[\leq 1]}, (\beta_1^{[\leq 1]})^2, g; l, \mu, 9, 0) = 0, \quad j = 1, 2, 3,$$

provided that $g = g_0^\pm$, with

$$g_0^\pm = (16 - \kappa^2)^{-1}(10\kappa \pm 41), \quad (\text{A } 3)$$

where we have introduced the parameterization (4.13) for μ . We note that the restriction $\kappa < 4$ will be sufficient for the moment. The choice of the g_0^- yields a larger range of variation for g as κ varies, which is much more convenient for actual applications. This implies that

$$\mathcal{J}_F := \frac{\partial(F_1, F_2, F_3)}{\partial(a_2, b_1, g)}(0, 2l(5 - \kappa)/9, g_0^-; \cdot) = \begin{pmatrix} 0 & 25 & \frac{2l(\kappa - 4)(\kappa + 4)}{9} \\ \frac{16l(5 - \kappa)}{9} & 0 & 0 \\ 0 & 4l(5 - \kappa) & \frac{4l^2(\kappa - 4)(\kappa + 4)}{9} \end{pmatrix}$$

is invertible under the condition $\kappa < 4$. Hence, by the Implicit Function Theorem, see, e.g. [40], the thesis follows. More precisely, for any given $l \in (0, 1)$, $\kappa < 4$ and $(m, \delta) \in (0, m_0) \times (0, \delta_0)$, the sequence $\mathbf{Z}^{(k)} := (z_1^{(k)}, z_2^{(k)})^\top$ defined by

$$\begin{cases} \mathbf{Z}^{(k+1)} &= \mathbf{Z}^{(k)} - \mathcal{M}F(\mathbf{Z}^{(k)}; l, \mu, \gamma, m) \\ \mathbf{Z}^{(0)} &= (2l(5 - \kappa)/9, g_0^-)^\top \end{cases}, \quad \mathcal{M} := \begin{pmatrix} (2\kappa)^{-1} & 0 & -(4l\kappa)^{-1} \\ \frac{9(\kappa - 5)}{2l\kappa(\kappa - 4)(\kappa + 4)} & 0 & \frac{45}{4l^2\kappa(\kappa - 4)(\kappa + 4)} \end{pmatrix} \quad (\text{A } 4)$$

satisfies the eigenvalue problem, i.e.

$$F(a_2(m), b_1(m, \delta), g(m, \delta); l, \mu, \gamma, m) = \mathbf{0},$$

recall (4.13), (4.16) and (A 2), where we have set

$$(b_1, g)(m, \delta) := \lim_{k \rightarrow +\infty} \mathbf{Z}^{(k)}.$$

The last step consists in computing the lower bound for κ stated in (4.13). The latter is obtained by requiring that (4.15) is satisfied. By taking into account (4.12), the first of (A 1) and

setting

$$\tilde{\alpha} := \mu l, \tag{A 5}$$

this condition is equivalent to require that

$$\mathcal{F} := \frac{g^2 \tilde{\alpha} - g + 2}{\sqrt{g^2 \tilde{\alpha}^2 + (4 - 2g)\tilde{\alpha} + 1}} - \frac{g}{2},$$

is strictly negative. By substituting $g = g_0^- = (9\tilde{\alpha})^{-1}(41 - 10\sqrt{16 - 9\tilde{\alpha}})$, one obtains up to the first order in m , and for all $\tilde{\alpha} \in (0, 16/9)$,

$$\mathcal{F}(\tilde{\alpha}) = \frac{5824 - 1476\tilde{\alpha} - 1460\sqrt{16 - 9\tilde{\alpha}} + \left(10\sqrt{16 - 9\tilde{\alpha}} - 41\right)\sqrt{-576\tilde{\alpha} - 640\sqrt{16 - 9\tilde{\alpha}} + 2624}}{18\tilde{\alpha}\sqrt{-576\tilde{\alpha} - 640\sqrt{16 - 9\tilde{\alpha}} + 2624}}.$$

It is easy to check that the latter is monotonically increasing on $[1/5, 2/5]$ and furthermore $\mathcal{F}(1/5)\mathcal{F}(2/5) < 0$, hence it possesses a unique zero on $(1/5, 2/5)$. More precisely, one can verify that $\mathcal{F}(\tilde{\alpha}) < 0$ for all $\tilde{\alpha} \in (1/5, 6/25)$ provided that m is sufficiently small. A comparison between (A 5) and (4.13) completes the proof, after a possible restriction of m_0 , if necessary.

Appendix B

(a) Expression of the coefficients γ_v

Let us denote with $C_{i,j}$ the elements of C and recall the definitions of h and d given in §3. The coefficients read as follows:

$$\begin{aligned} \gamma_{(3,0,0,0)} &= C_{2,1}^3 d - h C_{2,1}^2 C_{4,1} g + h C_{2,1}^2 C_{3,1}^2, \\ \gamma_{(0,3,0,0)} &= C_{2,2}^3 d - h C_{2,2}^2 C_{4,2} g + h C_{2,2}^2 C_{3,2}^2, \\ \gamma_{(0,0,3,0)} &= C_{2,3}^3 d + h C_{2,3}^2 (C_{3,3} - g C_{4,3}), \\ \gamma_{(0,0,0,3)} &= C_{2,4}^3 d + h C_{2,4}^2 (C_{3,4} - C_{4,4} g), \\ \gamma_{(1,1,1,0)} &= 6 C_{2,1} C_{2,2} C_{2,3} d - 2 h g (C_{2,1} C_{2,2} C_{4,3} - C_{2,1} C_{2,3} C_{4,2} - C_{2,2} C_{2,3} C_{4,1}) \\ &\quad + 2 h (C_{2,1} C_{2,2} C_{3,3} + C_{2,1} C_{2,3} C_{3,2} + C_{2,2} C_{2,3} C_{3,1}), \\ \gamma_{(1,0,1,1)} &= 6 C_{2,1} C_{2,3} C_{2,4} d - 2 h g (C_{2,1} C_{2,3} C_{4,4} - C_{2,1} C_{2,4} C_{4,3} - C_{2,3} C_{2,4} C_{4,1}) \\ &\quad + 2 h (C_{2,1} C_{2,3} C_{3,4} + C_{2,1} C_{2,4} C_{3,3} + C_{2,3} C_{2,4} C_{3,1}), \\ \gamma_{(0,1,1,1)} &= 6 C_{2,2} C_{2,3} C_{2,4} d - 2 h g (C_{2,2} C_{2,3} C_{4,4} - C_{2,2} C_{2,4} C_{4,3} - C_{2,3} C_{2,4} C_{4,2}) \\ &\quad + 2 h (C_{2,2} C_{2,3} C_{3,4} + C_{2,2} C_{2,4} C_{3,3} + C_{2,3} C_{2,4} C_{3,2}), \\ \gamma_{(0,0,1,2)} &= 3 C_{2,3} C_{2,4}^2 d - h g (C_{2,4}^2 C_{4,3} - 2 C_{2,3} C_{2,4} C_{4,4}) + h (C_{2,4}^2 C_{3,3} + 2 C_{2,3} C_{2,4} C_{3,4}), \\ \gamma_{(0,1,0,2)} &= 3 C_{2,2} C_{2,4}^2 d - h g (C_{2,4}^2 C_{4,2} - 2 C_{2,2} C_{2,4} C_{4,4}) + h (C_{2,4}^2 C_{3,2} + 2 C_{2,2} C_{2,4} C_{3,4}), \\ \gamma_{(1,0,0,2)} &= 3 C_{2,1} C_{2,4}^2 d - h g (C_{2,4}^2 C_{4,1} - 2 C_{2,1} C_{2,4} C_{4,4}) + h (C_{2,4}^2 C_{3,1} + 2 C_{2,1} C_{2,4} C_{3,4}), \\ \gamma_{(0,0,2,1)} &= 3 C_{2,3}^2 C_{2,4} d - h g (C_{2,3}^2 C_{4,4} - 2 C_{2,3} C_{2,4} C_{4,3}) + h (C_{2,3}^2 C_{3,4} + 2 C_{2,2} C_{2,4} C_{3,2}), \\ \gamma_{(2,0,1,0)} &= 3 C_{2,1}^2 C_{2,3} d - h g (C_{2,1}^2 C_{4,3} - 2 C_{2,1} C_{2,3} C_{4,1}), \\ \gamma_{(2,0,0,1)} &= 3 C_{2,1}^2 C_{2,4} d - h g (C_{2,1}^2 C_{4,4} - 2 C_{2,2} C_{2,4} C_{4,2}) + h (C_{2,1}^2 C_{3,4} + 2 C_{2,2} C_{2,4} C_{3,2}), \\ \gamma_{(0,1,2,0)} &= 3 C_{2,2}^2 C_{2,3} d - h g (C_{2,3}^2 C_{4,2} - 2 C_{2,2} C_{2,3} C_{4,3}) + h (C_{2,3}^2 C_{3,2} + 2 C_{2,2} C_{2,3} C_{3,3}), \\ \gamma_{(1,0,2,0)} &= 3 C_{2,1} C_{2,3}^2 d - h g (C_{2,3}^2 C_{4,1} - 2 C_{2,1} C_{2,3} C_{4,3}) + h (C_{2,3}^2 C_{3,1} + 2 C_{2,1} C_{2,3} C_{3,3}), \\ \gamma_{(0,2,1,0)} &= 3 C_{2,2}^2 C_{2,3} d - h g (C_{2,2}^2 C_{4,3} - 2 C_{2,2} C_{2,3} C_{4,2}) + h (C_{2,2}^2 C_{3,3} + 2 C_{2,2} C_{2,3} C_{3,2}), \\ \gamma_{(2,0,1,0)} &= 3 C_{2,1}^2 C_{2,3} d - h g (C_{2,1}^2 C_{4,3} - 2 C_{2,1} C_{2,3} C_{4,1}) + h (C_{2,1}^2 C_{3,3} + 2 C_{2,1} C_{2,3} C_{3,1}), \\ \gamma_{(1,2,0,0)} &= 3 C_{2,1} C_{2,2}^2 d - h g (C_{2,2}^2 C_{4,1} - 2 C_{2,1} C_{2,2} C_{4,2}) + h (C_{2,2}^2 C_{3,1} + 2 C_{2,1} C_{2,2} C_{3,2}) \\ \text{and} \quad \gamma_{(2,1,0,0)} &= 3 C_{2,1}^2 C_{2,2} d - h g (C_{2,1}^2 C_{4,2} - 2 C_{2,1} C_{2,2} C_{4,1}) + h (C_{2,1}^2 C_{3,2} + 2 C_{2,1} C_{2,2} C_{3,1}) \end{aligned} \tag{B 1}$$

Remark B.1. Note that h vanishes in the ‘zero dissipation limit’ with $\xi_1 = 0$.

References

- Romeo F, Ruzzene M. 2013 *Wave propagation in linear and nonlinear periodic media: analysis and applications*, vol. 540. Vienna, Austria: Springer Science & Business Media.
- Hussein MI, Leamy MJ, Ruzzene M. 2014 Dynamics of phononic materials and structures: historical origins, recent progress, and future outlook. *Appl. Mech. Rev.* **66**, 040802. (doi:10.1115/1.4026911)
- Muhammad, Lim C. 2022 From photonic crystals to seismic metamaterials: a review via phononic crystals and acoustic metamaterials. *Arch. Comput. Methods Eng.* **29**, 1137–1198. (doi:10.1007/s11831-021-09612-8)
- Andrianov IV, Danishevskyy V, Awrejcewicz J. 2021 *Linear and nonlinear waves in microstructured solids: homogenization and asymptotic approaches*. Boca Raton, FL: CRC Press.
- Fronk M, Fang L, Packo P, Leamy M. 2023 Elastic wave propagation in weakly nonlinear media and metamaterials: a review of recent developments. *Nonlinear Dyn.* **111**, 10709–10741. (doi:10.1007/s11071-023-08399-6)
- Patil G, Matlack K. 2022 Review of exploiting nonlinearity in phononic materials to enable nonlinear wave responses. *Acta Mech.* **233**, 1–46. (doi:10.1007/s00707-021-03089-z)
- Asfar O, Nayfeh A. 1983 The application of the method of multiple scales to wave propagation in periodic structures. *Siam Rev.* **25**, 455–480. (doi:10.1137/1025120)
- Lazarov BS, Jensen JS. 2007 Low-frequency band gaps in chains with attached non-linear oscillators. *Int. J. Non-Linear Mech.* **42**, 1186–1193. (doi:10.1016/j.ijnonlinmec.2007.09.007)
- Narisetti RK, Ruzzene M, Leamy MJ. 2012 Study of wave propagation in strongly nonlinear periodic lattices using a harmonic balance approach. *Wave Motion* **49**, 394–410. (doi:10.1016/j.wavemoti.2011.12.005)
- Narisetti RK, Leamy MJ, Ruzzene M. 2010 A perturbation approach for predicting wave propagation in one-dimensional nonlinear periodic structures. *J. Vib. Acoust.* **132**, 031001. (doi:10.1115/1.4000775)
- Narisetti RK, Ruzzene M, Leamy MJ. 2011 A perturbation approach for analyzing dispersion and group velocities in two-dimensional nonlinear periodic lattices. *J. Vib. Acoust.* **133**, 061020. (doi:10.1115/1.4004661)
- Campana MA, Ouisse M, Sadoulet-Reboul E, Ruzzene M, Neild S, Scarpa F. 2020 Impact of non-linear resonators in periodic structures using a perturbation approach. *Mech. Syst. Signal Process.* **135**, 106408. (doi:10.1016/j.ymsp.2019.106408)
- Chen Z, Zhou W, Lim C. 2020 Active control for acoustic wave propagation in nonlinear diatomic acoustic metamaterials. *Int. J. Non-Linear Mech.* **125**, 103535. (doi:10.1016/j.ijnonlinmec.2020.103535)
- Vakakis AF, King ME. 1995 Nonlinear wave transmission in a monocoupled elastic periodic system. *J. Acoust. Soc. Am.* **98**, 1534–1546. (doi:10.1121/1.413419)
- Manktelow K, Leamy MJ, Ruzzene M. 2011 Multiple scales analysis of wave–wave interactions in a cubically nonlinear monoatomic chain. *Nonlinear Dyn.* **63**, 193–203. (doi:10.1007/s11071-010-9796-1)
- Panigrahi SR, Feeny BF, Diaz AR. 2017 Second-order perturbation analysis of low-amplitude traveling waves in a periodic chain with quadratic and cubic nonlinearity. *Wave Motion* **69**, 1–15. (doi:10.1016/j.wavemoti.2016.11.004)
- Jiao W, Gonella S. 2019 Doubly nonlinear waveguides with self-switching functionality selection capabilities. *Phys. Rev. E* **99**, 042206. (doi:10.1103/PhysRevE.99.042206)
- Shen Y, Lacarbonara W. 2023 Nonlinearity enhanced wave bandgaps in metamaterial honeycombs embedding spider web-like resonators. *J. Sound Vibration* **562**, 117821. (doi:10.1016/j.jsv.2023.117821)
- Cummer SA, Christensen J, Alù A. 2016 Controlling sound with acoustic metamaterials. *Nat. Rev. Mater.* **1**, 16001. (doi:10.1038/natrevmats.2016.1)
- Ronellenfitch H, Stoop N, Yu J, Forrow A, Dunkel J. 2019 Inverse design of discrete mechanical metamaterials. *Phys. Rev. Mater.* **3**, 095201. (doi:10.1103/PhysRevMaterials.3.095201)
- Shen Y, Lacarbonara W. 2023 Nonlinear dispersion properties of metamaterial beams hosting nonlinear resonators and stopband optimization. *Mech. Syst. Signal Process.* **187**, 109920. (doi:10.1016/j.ymsp.2022.109920)

22. Georgiou IT, Vakakis AF. 1996 An invariant manifold approach for studying waves in a one-dimensional array of non-linear oscillators. *Int. J. Non-Linear Mech.* **31**, 871–886. (doi:10.1016/S0020-7462(96)00104-7)
23. Lepidi M, Bacigalupo A. 2019 Wave propagation properties of one-dimensional acoustic metamaterials with nonlinear diatomic microstructure. *Nonlinear Dyn.* **98**, 2711–2735. (doi:10.1007/s11071-019-05032-3)
24. Settini V, Lepidi M, Bacigalupo A. 2021 Nonlinear dispersion properties of one-dimensional mechanical metamaterials with inertia amplification. *Int. J. Mech. Sci.* **201**, 106461. (doi:10.1016/j.ijmecsci.2021.106461)
25. Silva P, Leamy M, Geers M, Kouznetsova V. 2019 Emergent subharmonic band gaps in nonlinear locally resonant metamaterials induced by autoparametric resonance. *Phys. Rev. E* **99**, 063003. (doi:10.1103/PhysRevE.99.063003)
26. Panigrahi SR, Feeny BF, Diaz AR. 2017 Wave–wave interactions in a periodic chain with quadratic nonlinearity. *Wave Motion* **69**, 65–80. (doi:10.1016/j.wavemoti.2016.11.008)
27. Andrianov IV, Danishevskyy VV, Rogerson G. 2020 Vibrations of nonlinear elastic lattices: low-and high-frequency dynamic models, internal resonances and modes coupling. *Proc. R. Soc. A* **476**, 20190532. (doi:10.1098/rspa.2019.0532)
28. Fronk MD, Leamy MJ. 2019 Internally resonant wave energy exchange in weakly nonlinear lattices and metamaterials. *Phys. Rev. E* **100**, 032213. (doi:10.1103/PhysRevE.100.032213)
29. Fortunati A, Bacigalupo A, Lepidi M, Arena A, Lacarbonara W. 2022 Nonlinear wave propagation in locally dissipative metamaterials via Hamiltonian perturbation approach. *Nonlinear Dyn.* **108**, 765–787. (doi:10.1007/s11071-022-07199-8)
30. Giorgilli A. 2003 Exponential stability of Hamiltonian systems. In *Dynamical systems. Part I Pubbl. Cent. Ric. Mat. Ennio Giorgi*, pp. 87–198. Scuola Norm. Sup., Pisa.
31. Berdichevsky V. 2009 *Variational principles of continuum mechanics: I. Fundamentals*. Berlin, Heidelberg: *Interaction of Mechanics and Mathematics*. Springer.
32. Ferraz-Mello S. 2007 *Canonical Perturbation Theories: Degenerate Systems and Resonance*. New York, NY: Springer Science & Business Media.
33. Giorgilli A, Galgani L. 1978 Formal integrals for an autonomous Hamiltonian system near an equilibrium point. *Cel. Mech.* **17**, 267–280. (doi:10.1007/BF01232832)
34. Carboni B, Arena A, Lacarbonara W. 2021 Nonlinear vibration absorbers for ropeway roller batteries control. *Proc. Inst. Mech. Eng., Part C: J. Mech. Eng. Sci.* **235**, 4704–4718. (doi:10.1177/0954406220953454)
35. Fortunati A, Wiggins S. 2016 Integrability and strong normal forms for non-autonomous systems in a neighbourhood of an equilibrium. *J. Math. Phys.* **57**, 092703. (doi:10.1063/1.4962802)
36. Shilnikov LP, Shilnikov AL, Turaev DV, Chua LO. 1998 *Methods of Qualitative Theory in Nonlinear Dynamics*, vol. I. World Scientific Series on Nonlinear Science. Series A.
37. Arnold VI, Kozlov VV, Neishtadt AI. 2006 *Mathematical aspects of classical and celestial mechanics*. Encyclopaedia of Mathematical Sciences. Springer Berlin Heidelberg.
38. Lacarbonara W, Camillacci R. 2004 Nonlinear normal modes of structural systems via asymptotic approach. *Int. J. Solids Struct.* **41**, 5565–5594. (doi:10.1016/j.ijsolstr.2004.04.029)
39. Braun M. 1993 *Differential equations and their applications: an introduction to applied mathematics*. Applied Mathematical Sciences. New York, NY: Springer.
40. Krantz SG, Parks HR. 2013 *The implicit function theorem: history, theory, and applications*. Modern Birkhäuser Classics. New York, NY: Springer.